Reinforced geopolymer cement concrete in flexure: A closer look at stress-strain performance and equivalent stress-block parameters

Brett Tempest, Janos Gergely, and Ashley Skipper

- Geopolymer cement concrete could revolutionize the concrete industry by merging the benefits of concrete with significantly reduced greenhouse gas emissions compared with portland cement concrete.
- The research presented in this paper used a combined axial stress and flexure test developed by Hognestad et al. as a primary means of determining the distribution of stresses in the compression zone of geopolymer cement concrete in flexure.
- The results indicated that slightly modified stress block parameters α_1 and β_1 should be applied to geopolymer cement concrete due to differences in the stress-strain relationship of geopolymer cement concrete in compression compared with portland cement concrete.

Concrete has achieved its status as the most widely used building material in the world because of its versatility, strength, and durability. However, the production of portland cement is an emissions-intensive process that accounts for approximately 5% of global carbon dioxide emissions.[1] Geopolymer cement, first named and described by Davidovits,[2] is an alternative to portland cement as a binder in concrete. Critical analyses of geopolymer and portland cements have estimated the reduction in carbon dioxide associated with geopolymer cement to be as high as 80% and as low as 9%.[3,4] Other studies have indicated that, depending on the industrial processes used and the source material locations, emissions associated with geopolymer cement concrete can range from 97% lower to 14% higher than those of portland cement concrete.[5] The potential to reduce the carbon dioxide emissions associated with concrete production is sufficient incentive to motivate the wider-scale adoption of geopolymer cement concrete technologies as a climate change mitigation strategy.

Some examples of full-scale facilities built with geopolymer cement concrete demonstrate that there has been sufficient advancement of the technology to enable real-world engineering and construction.[6] Van Deventer has described a path to industrialization that includes demonstration projects and the development of specific standards for

geopolymer cement concrete.[7] In order to encourage more widespread production and adoption of geopolymer cement concrete materials in routine construction, their engineering properties and performance in typical structural components must be determined experimentally and documented. Any significant differences between the performance of geopolymer cement concrete and portland cement concrete must be highlighted so that future editions of building code requirements can accurately govern the design with geopolymer materials. Similarities in the performance of the two materials could enable the use of existing codes and provisions.

Prior research works by Sumajouw and Rangan[8] and Yost et al.[9] compared observations from destructive beam tests with estimates made using existing design parameters published by the American Concrete Institute (ACI 318-14)[10] and Standards Australia (AS 3600)[11] and determined that they provide sufficient accuracy for design purposes. However, Prachasaree et al.[12] highlighted the need for geopolymer-cement-concrete-specific design parameters due to differences in the deformational behavior compared with that of portland cement concrete. This paper describes the evaluation of compressive flexural performance of geopolymer cement concrete using test methods devised by Hognestad et al.[13] to evaluate the stress distribution in concrete beams near ultimate conditions. The results are then applied to predict the strength of a series of reinforced geopolymer cement concrete beams that were tested to failure.

Background

Davidovits[14] describes four general types of geopolymer cements: slag-based, rock-based, fly-ash-based, and ferrosialate-based. Geopolymer cements sourced from fly ash require an activating solution, often composed of sodium silicate and sodium hydroxide, in order to develop cementitious properties in the fly ash.[14] The activating solution and fly ash are combined with aggregates to produce concrete. Water and superplasticizer may also be added to improve the workability of the concrete mixture. The use of fly-ash-based geopolymers as a binder typically requires the concrete to be cured at an elevated temperature of 140°F to 176°F (60°C to 80°C) for up to 48 hours.[15,16] Geopolymer cement concrete develops its full compressive strength through this heat-curing process.

Several recent experimental studies have been performed to evaluate the material properties and structural performance of geopolymer cement concrete and have shown that these characteristics are similar to those of portland cement concrete. Diaz-Loya et al.[17] studied the static elastic modulus, compressive strength, modulus of rupture, and Poisson's ratio of 25 batches of geopolymer cement concrete. The elastic modulus ranged from 988 to 6219 ksi (6.81 to 42.9 GPa), compressive strengths ranged from 1500 to 11,657 psi (10.3 to 80.4 MPa), the modulus of rupture ranged from 397 to 929 psi (2.74 to 6.41 MPa), and the average Poisson's ratio was 0.14.

Despite these general similarities between the physical characteristics of geopolymer cement concrete and portland cement concrete, there are also significant differences that may affect the decision to use design parameters developed for portland cement concrete. The elastic modulus is generally lower, and shrinkage and creep phenomena occur at a reduced magnitude.[18] In addition, the tensile strength of geopolymer cement concrete materials may be slightly greater than would be expected for portland cement concrete with similar compressive strength.[6] These characteristics and their impacts on beam strength and deflection are described by Tempest.[18]

Thomas and Peethemparan[19] investigated the stress-strain relationship of alkali-activated cement concretes prepared with either slag cement or high-calcium fly ash. Using uniaxial compression tests, the team measured the stress-strain relationship in the linear elastic, softening, and post-peak loading phases. The performance up to peak stress correlated well with models for the stress-strain relationship in portland cement concrete, with similar compressive strength and elastic modulus. A significant difference relative to portland cement concrete was the tendency of alkali-activated cement concrete to display brittle fracture immediately after peak stress was reached.

Cross et al.[20] reported the behavior of reinforced geopolymer cement concrete beams undergoing four-point bending to determine the validity of current design methodology for portland cement concrete beams. Three reinforced geopolymer cement concrete beams were designed and fabricated according to the design methodology in ACI 318-14 for portland cement concrete. During testing, the beams showed a ductile response, with the tensile steel yielding followed by crushing of the compression concrete. The observed ultimate moments for all three beams were higher than the moment capacity as calculated using the provisions of ACI 318-14.

Sumajouw and Rangan[8] investigated the flexural behavior of reinforced geopolymer cement concrete beams and evaluated the strength, crack pattern, deflections, and ductility to verify the use of existing portland cement concrete design provisions in AS 3600 with geopolymer cement concrete. A series of 12 reinforced geopolymer cement concrete beams were fabricated and tested with variations in the longitudinal tensile reinforcement ratio and the compressive strength of the specimens. The reinforced beams were designed with compressive strengths of 5800, 7300, and 10,800 psi (40, 50, and 75 MPa). The ratio of observed capacity to predicted capacity averaged 1.11 for all of the specimens, demonstrating that the code provisions are applicable to estimating the capacity of geopolymer cement

concrete beams. The ratio of observed-to-predicted deflection measurements averaged 1.15, which suggests that the provisions of AS 3600 also accurately and conservatively predict the serviceability of reinforced geopolymer cement concrete beams.

Yost et al.[9] investigated the behavior of reinforced geopolymer cement concrete beams under the influence of four-point bending. As in previously reported studies, the observations showed that the underreinforced geopolymer cement concrete beams behaved similarly to the underreinforced portland cement concrete beams. The geopolymer cement concrete beams demonstrated a more sudden failure and explosive response than the portland cement concrete beams. The geopolymer cement concrete beams also developed a higher concrete strain at compression failure than the portland cement concrete beams. The average concrete strains were 3147 and 3373 $\mu\varepsilon$ for the underreinforced geopolymer cement concrete and portland cement concrete beams, respectively. The overreinforced geopolymer cement concrete beams also showed a more sudden failure in comparison to the similarly designed portland cement concrete beams. The underreinforced geopolymer cement concrete beams had an average observed-to-predicted ratio of 1.26, which was slightly higher than the 1.19 ratio for the underreinforced portland cement concrete specimens.

The summary consensus of studies that have compared experimental results of beam tests with strength predictions is that existing ACI parameters yield acceptable results. This has been generally true for underreinforced beams with small cross sections that make up the bulk of the beams reported in the literature. The risk of mischaracterizing the stress distribution within the compression zone of a beam in flexure is low for beams with shallow neutral axes. However, beams with greater reinforcement ratios ρ or lower-strength concrete have deeper compressive stress zones at failure. In these cases, the actual stress distribution, and therefore the more accurate shape of the equivalent stress block, can cause larger errors if not assumed correctly. **Figure 1** illustrates this relationship. The nominal moment capacity of a hypothetical 16 × 24 in. (410 × 610 mm) beam with concrete compressive strength from 3000 to 12,000 psi (21 to 83 MPa) is plotted with reinforcement ratios up to ρ_{bal} (the reinforcement ratio at balanced failure conditions). Increasing or decreasing the value of the stress block parameter α_1 (that is, 0.85 for 4000 psi [27.6 MPa] concrete) by 10% leads to little change in the estimated moment capacity for beams with low ρ. However, at ρ_{bal}, the range of the results can be up to approximately 7% of the total beam strength, as in the 3000 psi beam. This indicates that more-exact parameters are required for more heavily reinforced beams, especially if they are significantly deep and do not use high-strength concrete.

Prachasaree et al.[12] approached the problem of developing geopolymer-cement-concrete-specific stress-block parameters with analytical methods. The group used data from tests of the elastic characteristics of geopolymer cement concrete to analytically determine the parameters of an equivalent stress block particular to geopolymer cement concrete. Using this information, a general stress-strain relationship for geopolymer cement concrete was created and compared with research from other authors. The team found that the stress-block parameters given in ACI 318-14 for use in portland cement concrete design were not appropriate for reinforced geopolymer cement concrete design and proposed values based on the tests of geopolymer cement concrete materials. The resulting parameters yielded better estimates of beam capacity.

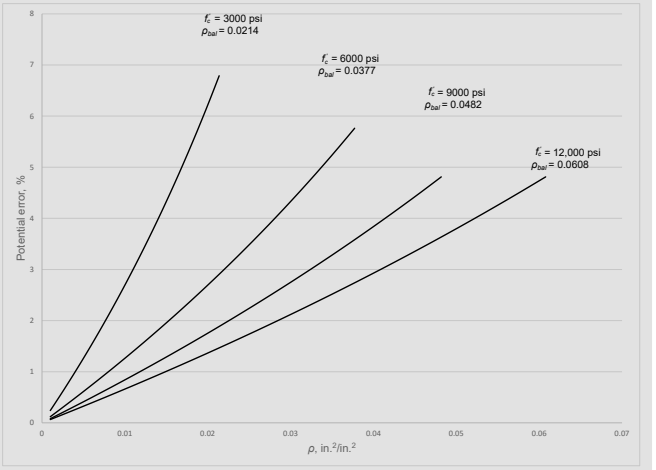

Figure 1. Potential error from inaccurate stress-block parameters in beams with higher reinforcement ratios. Note: f'_c = compressive strength of concrete; ρ = reinforcement ratio; ρ_{bal} = reinforcement ratio at balanced failure conditions. 1 in. = 25.4 mm; 1 psi = 6.895 kPa.

Based on the findings of the initial research performed by Tempest,[18] a second study was launched by Skipper and Tempest to establish stress-strain relationships for geopolymer cement concrete in flexure using bending tests rather than uniaxial compression.[21] These tests established the stress-block parameters α_1 and β_1 that are specific to geopolymer cement concrete of various compressive strengths. The outcome of these tests is presented in the following sections.

Research objectives and methods

The studies listed in the review of previous research related to the flexural performance of reinforced geopolymer cement concrete verify the applicability of various portland cement concrete design provisions to geopolymer cement concrete. This paper presents results of experiments conducted to directly determine parameters α_1 and β_1 that define the equivalent compressive stress block that is commonly used for concrete design purposes. The cross-hatched area in **Fig. 2** represents the compression zone of a beam in positive moment flexure. The strain distribution for this segment of the cross section is linear (Fig. 2);

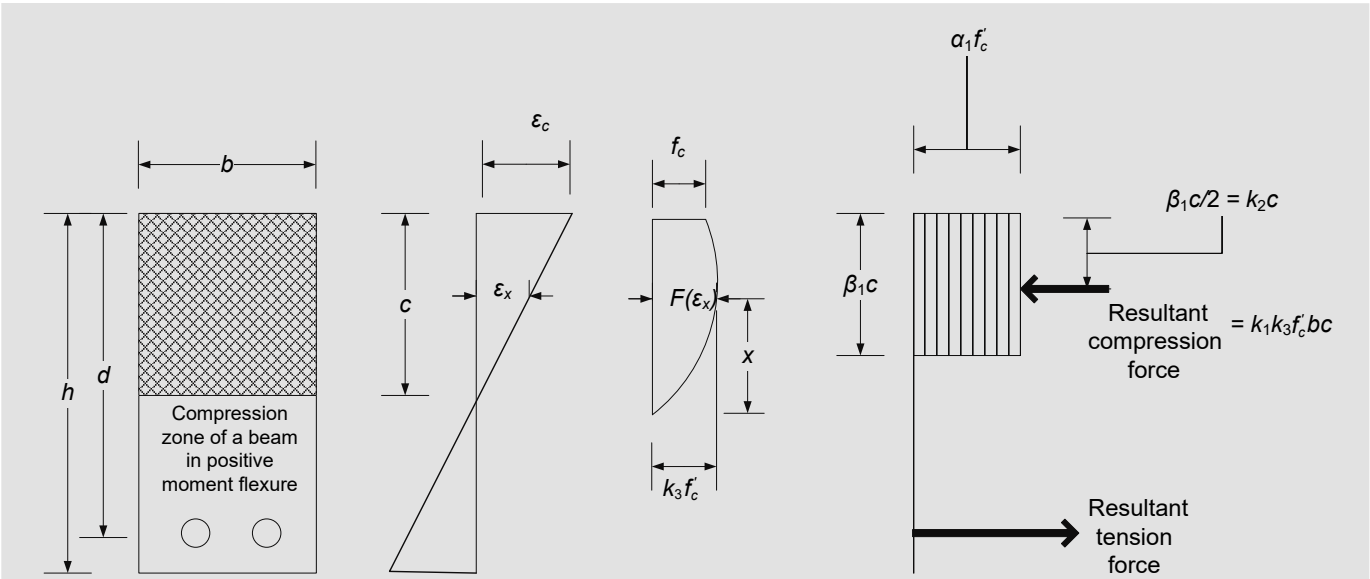

Figure 2. Stresses and strains in concrete beams, relationship of k_1, k_2, and k_3 to the resultant compressive force. Note: b = width of a rectangular concrete section; c = distance from the compressive face to the neutral axis in a concrete beam; C = resultant compressive force; d = distance from the extreme compression fiber to the centroid of the compression reinforcing steel group; f_c = stress in the concrete; f_c' = compressive strength of concrete; F = forces acting on the section of the beam column; h = depth of beam; k_1 = ratio of average compressive stress to maximum compressive stress; k_2 = ratio of distance from top of beam to the resultant compressive force C and the depth to the neutral axis c; k_3 = ratio of cylinder concrete strength to beam concrete strength; x = distance from neutral axis to the resultant compressive force line of action; α_1 = stress-block parameter; β_1 = stress-block parameter; ε_c = concrete strain; ε_x = unknown concrete strain.

however, these strains do not have a linear relationship to stresses after the concrete begins to crack and soften. Beams approaching their capacity in flexure would contain the stress distribution in Fig. 2. For design purposes, the Whitney stress block (Fig. 2) is used as an approximation of the area enclosed by the parabolic area.[22] The block is defined by the factors in Fig. 2, where

k_1 = ratio of average compressive stress to maximum compressive stress

k_2 = ratio of distance from top of beam to the resultant compressive force C and the depth to the neutral axis c

k_3 = ratio of cylinder concrete strength to beam concrete strength

There are several challenges in determining experimentally the stress-strain relationship in Fig. 2. Although concentric compression tests can be used to determine the stress-strain relationship through the initiation of crushing, the postpeak behavior is typically obscured by the rapid release of strain energy stored in the testing device. For the purpose of estimating k_1, k_2, and k_3, as well as measuring the stress-strain relationship, a combined axial-flexure test was developed by Hognestad et al.[13] In this procedure, a short beam column is loaded axially, while an eccentric load is applied through two arms attached to the ends of the specimen (shown cut across an axis of vertical symmetry in **Fig. 3**). The eccentric load produces a moment that maintains a neutral face on one side of the beam column while the opposite side approaches the compressive strain limit. In this way, the area between the compression face and the neutral axis of the flexural beam is simulated without the effects of tensile stresses and a shifting neutral axis, as would be found in a reinforced beam. Because this is not possible in concentric tests, the stress and strain gradients that are found in flexural components are duplicated in the test piece. **Figure 3** shows the test geometry, with P_1 representing the primary axial load and P_2 representing the eccentric load.

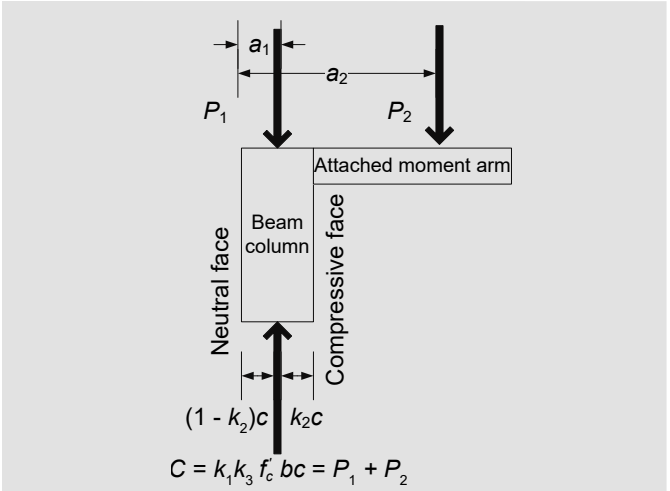

Figure 3. Free body diagram of the beam-column specimen cut at midheight. Note: a_1 = distance from the neutral face to P_1; a_2 = distance from the neutral face to P_2; b = width of a rectangular concrete section; c = distance from the compressive face to the neutral axis in a concrete beam; C = resultant compressive force; f_c' = compressive strength of concrete; k_1 = ratio of average compressive stress to maximum compressive stress; k_2 = ratio of distance from top of beam to the resultant compressive force C and the depth to the neutral axis c; k_3 = ratio of cylinder concrete strength to beam concrete strength; P_1 = primary axial load acting on the beam column; P_2 = eccentric load acting on the beam column.

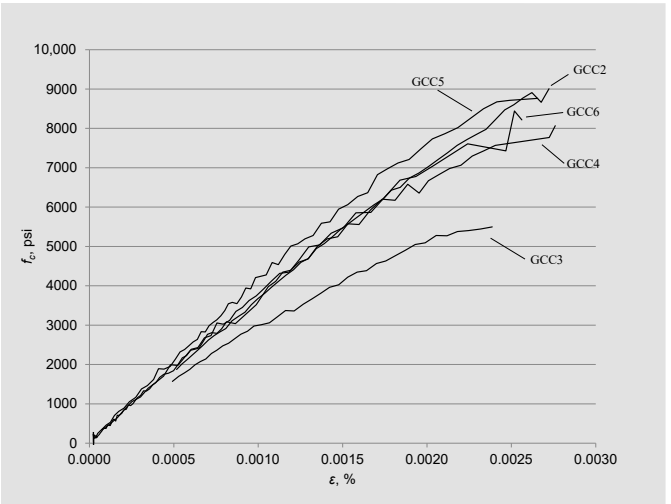

Figure 4. Relative slopes of stress-strain curves. Note: f_c = stress in the concrete; ε = strain. 1 psi = 6.895 kPa.

Based on static analysis of the system, k_1k_3 and k_2 can be calculated directly from the beam dimensions and the magnitude of the loads P_1 and P_2 (Fig. 3). The resultant compressive force C of the stress in the concrete (Fig. 3) is equal to the sum of the applied forces P_1 and P_2. Equation (1) results from the free body diagram given in Fig. 3.

$$\sum F = 0 = k_1 k_3 f_c' bc - (P_1 + P_2) \tag{1}$$

where

F = forces acting on the section of the beam column

f_c' = compressive strength of concrete

b = width of a rectangular concrete section

c = distance from the compressive face to the neutral axis in a concrete beam

Solving for k_1k_3 gives Eq. (2).

$$k_1 k_3 = \frac{(P_1 + P_2)}{f_c' bc} \tag{2}$$

Taking the sum of the moments about the neutral face of the beam generated by the forces shown in Fig. 5 gives Eq. (3), which is solved for k_2 in Eq. (4).

$$\sum M = 0 = (P_1 + P_2)(1 - k_2)c - P_1 a_1 - P_2 a_2 \tag{3}$$

where

M = moment

a_1 = distance from the neutral face to P_1

a_2 = distance from the neutral face to P_2

$$k_2 = 1 - \frac{P_1 a_1 - P_2 a_2}{(P_1 + P_2)c} \tag{4}$$

The relationship between stress and strain must be determined by a process of numerical integration. It is necessary to assume that the stress in the concrete f_c is a function of ε_x, where ε_x is a linear distribution across c (Fig. 2). However, because the function $F(\varepsilon_x)$ is not known, some substitution of known or measurable quantities must be made to determine f_c from data collected during experiments.

The resultant compressive force C may be defined by Eq. (5).

$$C = b\int_0^c F(\varepsilon_x)dx = \frac{bc}{\varepsilon_c}\int_0^{\varepsilon_c} F(\varepsilon_x)d\varepsilon_x = P_1 + P_2 = f_0 bc \tag{5}$$

where

ε_c = concrete strain

f_0 = average stress on a cross section of the beam column

The moment M is determined by Eq. (6).

$$\begin{aligned} M &= b\int_0^c F(\varepsilon_x)x dx = \frac{bc^2}{\varepsilon_c^2}\int_0^{\varepsilon_c} F(\varepsilon_x)\varepsilon_x d\varepsilon_x \\ &= P_1 a_1 + P_2 a_2 = m_0 bc^2 \end{aligned} \tag{6}$$

where

m_0 = average moment acting on a section of the beam column

Equation (7) calculates the average stress on the cross section f_0.

$$f_0 = \frac{P_1 + P_2}{bc} \tag{7}$$

Eq. (8) determines the average moment m_0.

$$m_0 = \frac{P_1 a_1 - P_2 a_2}{bc^2} \tag{8}$$

Differentiating the third and last terms of Eq. (5) with

respect to ε_c results in Eq. (9). Substituting the relationship in Eq. (10), which is obtained by manipulating the third and fifth terms of Eq. (5) into Eq. (9), where $\frac{df_0}{d\varepsilon_c}$ is approximately equal to $\frac{\Delta f_0}{\Delta \varepsilon_c}$, two quantities that are measured during testing. The unknown function $F(\varepsilon_x)$ has been removed from the analysis, permitting the measured quantities P_1, P_2, and ε_c to be used to directly calculate f_c.

$$\int_0^{\varepsilon_c} F(\varepsilon_x)\, d\varepsilon_x = f_0 \varepsilon_c \tag{9}$$

$$f_c = \frac{df_0}{d\varepsilon_c}\varepsilon_c + f_0 \tag{10}$$

Using the same strategy gives Eq. (11).

$$f_c = \frac{dm_0}{d\varepsilon_c}\varepsilon_c + 2m_0 \tag{11}$$

Specimen preparation

To conduct the flexural test to collect the quantities described previously, five beam columns and five reinforced beams were constructed. The beam columns featured an unreinforced geopolymer cement concrete cross section that was 7.25 in. (184 mm) deep in the transverse dimension and 7.5 in. (190 mm) deep in the direction perpendicular to the bending axis. The formwork was constructed of ¾ in. (19 mm) oriented strand board and was heavily stiffened with extra framing in order to maintain its geometry under the pressure of the fresh concrete. The forms were also lined with polyethylene sheeting in order to prevent the absorption of water or the alkaline activator into the wood. Sleeves fabricated from square, hollow structural steel were cast onto each end of the specimen. The holes were precisely located to accommodate the bolting pattern of the moment arms. Passages for the bolts were blocked out with lengths of polyvinyl chloride pipe that were removed after the concrete cured. Bent hoops of Grade 60 (414 MPa), no. 3 (10M) reinforcing bar provided reinforcing inside of the sleeve. No. 4 (13M) bars extended a short distance beyond the end of the sleeve to transfer forces from the loaded ends of the beam column into the unreinforced central portion of the specimen.

Table 1 lists the materials in the concrete mixture design used to cast the reinforced concrete beams and the beam columns. The fly ash used was marketed as ASTM C618 Class F, which originated from a steam generation plant in the southeastern United States. The cementitious materials also included sodium hydroxide pellets. Specimens GCC1 through GCC3 contained sodium silicate solution as a source of soluble silica in the activating solution. Specimens GCC4 through GCC7 contained silica fume as the supplemental source of soluble silica. Coarse aggregates used were a granite type conforming to ASTM C33-16 size 7, with 0.5 in. (13 mm) maximum particle diameter. The fine aggregate was silica sand, which also met ASTM C33-16 requirements for concrete applications. Table 1 also shows the strength of companion cylinders cast with the beam columns. The cylinders were tested at the same time as their associated beam or beam column. Because the two types of specimens were tested at different concrete ages, there was typically some strength gain

Table 1. Geopolymer cement concrete mixture designs

	GCC1	GCC2	GCC3	GCC4	GCC5	GCC6	GCC7
Fly ash, lb/yd^3	785	787	787	834	834	834	834
Water, lb/yd^3	286	245	245	275	274	280	28
Sodium hydroxide, lb/yd^3	31	36	36	83	83	83	83
Silica fume, lb/yd^3	0	0	0	62	62	62	62
Sodium silicate, lb/yd^3	93	107	107	0	0	0	0
Fine aggregate, lb/yd^3	1452	1370	1370	1336	1336	1336	1336
Coarse aggregate, lb/yd^3	1391	1370	1370	1336	1336	1336	1336
w/cm	0.31	0.26	0.26	0.28	0.28	0.29	0.29
Beam f_c', psi	3200	6000	n/a	n/a	n/a	n/a	11,900
Beam column f_c', psi	Not tested	7000	5200	7900	9000	7300	n/a

Note: f_c' = compressive strength of concrete; n/a = not applicable (not tested); *w/cm* = water–cementitious materials ratio. 1 psi = 6.895 kPa; 1 lb/yd^3 = 0.593 kg/m^3.

between the beam test and the beam-column tests. Test specimens GCC1, GCC2, and GCC3 were prepared in a precast concrete plant setting, and the concrete mixing was provided by a 10 yd^3 (7.6 m^3) capacity mixing truck.[6] Specimens GCC4, GCC5, and GCC6 were prepared in a university lab setting and were mixed in a 3 ft^3 (0.085 m^3) rotary mixer. Specimen GCC7 was prepared in a university lab setting but was mixed in a 10 yd^3 (7.65 m^3) capacity mixing truck.[6]

The mixture proportions for specimens GCC4 through GCC7 were similar (Table 1), but small variations in the water content caused differences in the compressive strength of the concrete. After casting, the specimens were allowed a 48-hour aging period at ambient temperature. Following aging, the specimens were cured for 48 hours in a 167°F (75.0°C) oven constructed with rigid insulation panels and conditioned by electric resistance space heaters.

The specimens were instrumented with five concrete strain gauges. Two gauges were mounted on the compression face of the beam column, and two were mounted on the neutral face within 2 in. (50 mm) of the centerline. The primary axial load P_1 was applied at a rate of approximately 20 kip/min (89 kN/min). The moment was applied through the arms by an actuator controlled by a closed-loop routine.

During the testing process, measurements were recorded by a data acquisition system set to measure twice per second. The system recorded the loads P_1 and P_2, strain from each of the five strain gauges, and displacement at the inside and outside of the beam at midspan. The displacement data recorded during the test was used to compute additional stresses caused by secondary moments related to P_1 and P_2 acting through the eccentricity e. These additional stresses were calculated by Eq. (12), which is a modification of Eq. (8).

To accommodate a force limitation in the testing apparatus, the cross sections of beam-column specimens GCC2 and GCC3 were slightly reduced by saw cutting 1 in. (25 mm) vertical slits into the specimen at midspan. Specimens typically failed by initiating crushing at the compression face. At the end of the test, sufficient cross section had been lost from the specimens that the initially concentric P_1 force became eccentric and the specimens usually failed in shear.

Discussion of beam-column results

The five beam-column specimens provided a spectrum of stress-strain response that appears to be related to concrete compressive strength. The slope of the stress-strain curve increases as the concrete compressive strength increases (**Fig. 4**). **Figure 5** represents the correlation between the slope of the stress-strain relationship (Fig. 4) and the concrete compressive strength f_c'. Analogous to portland cement concrete, the relationship between compressive strength and elastic modulus E_c can be represented by Eq. (13).

$$E_c = \psi \sqrt{f_c'} \tag{13}$$

where

ψ = factor fit to the data

For normalweight portland cement concrete, the factor ψ in Eq. (13) is commonly accepted as equal to 57,000 (4700 for SI units). In the case of the results presented here, ψ equals 43,000 (3575 for SI units) and fits the data with coefficient of determination R^2 equal to 0.99. This elastic modulus is similar to that of portland cement concrete with lightweight aggregate.

Analysis of beam-column test data

Equations (2) and (4) allow the computation of k_1k_3 and k_2, respectively. **Table 2** presents the results of these calculations using test data as inputs. The mixtures for specimens GCC1 and GCC6 were not successfully tested due to equipment malfunctions. The ratio of cylinder concrete strength to beam concrete strength k_3 was found as the ratio of f_c' to the maximum concrete stress f_c determined during the test. The parameters of α_1 and β_1 were calculated using Eq. (14) and (15).

$$\alpha_1 = \frac{k_1k_3}{2k_2} \tag{14}$$

$$\beta_1 = 2k_2 \tag{15}$$

Figures 6 and **7** show the relationship of α_1 and β_1 to the cylinder compressive strength of the concrete in the beam

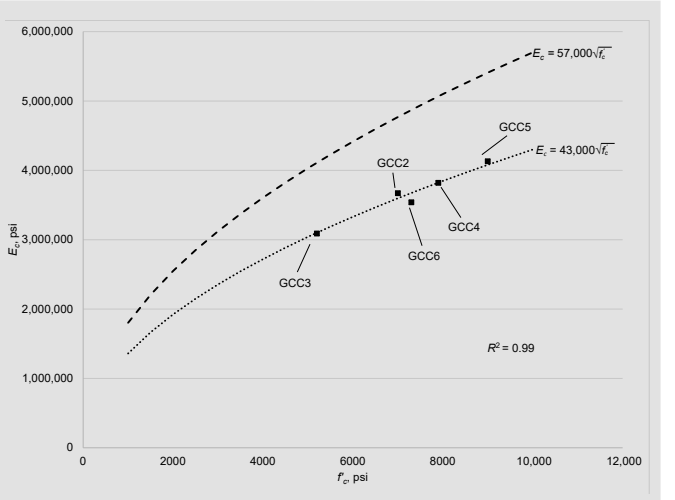

Figure 5. Relationship of compressive strength to modulus of elasticity. Note: E_c = elastic modulus of the concrete; f_c' = compressive strength of concrete; R^2 = coefficient of determination. 1 psi = 6.895 kPa.

Table 2. Calculated values of k_1, k_2, and k_3 for beam columns

Specimen	f_c', psi	E_c, psi	k_1k_3	k_1	k_2	k_3	α_1	β_1
GCC2	7000	3,670,000	0.683	0.61	0.347	1.11	0.98	0.69
GCC3	5200	3,090,000	0.614	0.58	0.346	1.06	0.89	0.69
GCC4	7900	3,820,000	0.513	0.5	0.228	1.03	1.13	0.46
GCC5	9000	4,130,000	0.519	0.53	0.231	0.98	1.12	0.46
GCC6	7300	3,760,000	0.593	0.54	0.275	1.1	1.08	0.55

Note: E_c = elastic modulus of the concrete; f_c' = compressive strength of concrete; k_1 = ratio of average compressive stress to maximum compressive stress; k_2 = ratio of distance from top of beam to the resultant compressive force C and the depth to the neutral axis c; k_3 = ratio of cylinder concrete strength to beam concrete strength; α_1 = stress-block parameter = $\frac{k_1k_3}{2k_2}$; β_1 = stress-block parameter = $2k_2$. 1 psi = 6.895 kPa.

columns, respectively. All α_1 were in the range of 1.0, with an upper bound of 1.13 and a lower bound of 0.89. Although Fig. 6 indicates that α_1 varies with concrete strength, the variation is not pronounced. The preponderance of values above 1.0 implies that the compressive strength of concrete in large components is greater than the compressive strength in small test cylinders. This is most likely an indication of improved curing of concrete in massive components over concrete in cylinders. Because the curing process is improved by heating, the larger items benefit from their larger heat storage capacity. This phenomenon should be investigated further.

Also, differences in the compressive strength of the specimens with similar mixture designs could also be related to temperature variations at different locations in the curing oven. There are not sufficient data to justify proposing a design value of α_1 based on the cylinder compressive strength until further research can illuminate the causes of this difference. However, although α_1 is taken as 0.85 for all cases with portland cement concrete, there may be reason to relate α_1 to specimen size or shape for geopolymer cement concrete materials. Alternatively, more sophisticated curing of test cylinders could be used to better relate the compressive strength of a cylinder with the compressive strength of concrete placed in a structural component. Based on the results of these tests, the relationship shown in Eq. (16) is proposed to relate α_1 to f_c'.

$$\alpha_1 = (7 \times 10^{-5})f_c' + 0.5486 \quad (16)$$

Figure 7 plots β_1, which shows a tendency to be slightly reduced as cylinder compressive strength increases. For normal-strength portland cement concrete, ACI 318-14 provides a range for β_1 of 0.85 for concrete between 2500 and 4000 psi (17 and 27 MPa) to β_1 of 0.65 for concrete above 8000 psi (55 MPa). The beam-column specimens tested ranged in strength from 5200 to 9000 psi (36 to 62 MPa); however, the range of β_1 values was not nearly as broad. For the geopolymer cement concrete beam-column specimens, β_1 values ranged from 0.69 for the 5200 psi concrete to 0.46 for the higher-strength concrete. The

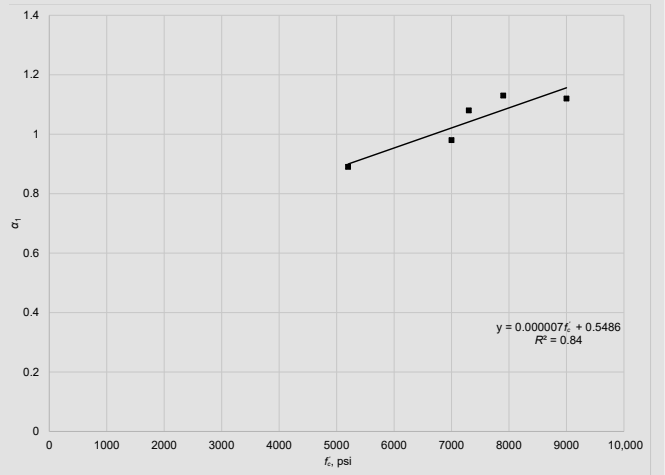

Figure 6. Stress-block parameter α_1 related to cylinder compressive strength for beam columns. Note: f_c' = compressive strength of concrete; R^2 = coefficient of determination. 1 psi = 6.895 kPa.

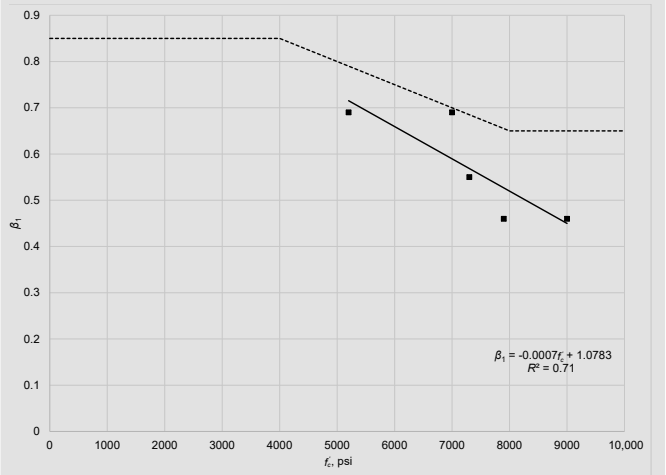

Figure 7. Stress-block parameter β_1 related to cylinder compressive strength for beam columns. Note: f_c' = compressive strength of concrete; R^2 = coefficient of determination. 1 psi = 6.895 kPa.

Table 3. Reinforcement details, dimensions, and material properties for analysis of beam capacity

Beam	Source	A_s', in.^{2}	A_s, in.^{2}	d', in.	d, in.	f_y, psi	f_c', psi
1	GCC1-beam1	0.40	0.60	1.0	11.0	82,000	3200
2	GCC1-beam2	0.40	0.60	1.0	11.0	82,000	3200
3	GCC2-beam1	0.40	0.60	1.0	11.0	90,000	6000
4	GCC2-beam2	0.40	0.60	1.0	11.0	90,000	6000
5	GCC7-beam1	0.40	0.60	3.0	11.0	80,000	11,900
6	Sumajouw	0.35	0.53	1.7	10.1	79,771	5366
7	Sumajouw	0.35	0.93	1.7	10.0	81,221	6092
8	Sumajouw	0.35	1.46	1.7	10.0	81,221	6092
9	Sumajouw	0.35	2.10	1.7	9.9	80,786	5366
10	Sumajouw	0.35	0.53	1.7	10.1	79,771	6672
11	Sumajouw	0.35	0.93	1.7	10.0	81,221	7687
12	Sumajouw	0.35	1.46	1.7	10.0	81,221	7687
13	Sumajouw	0.35	2.10	1.7	9.9	80,786	6672
14	Sumajouw	0.35	0.53	1.7	10.1	79,771	11,023
15	Sumajouw	0.35	0.93	1.7	10.0	81,221	10,443
16	Sumajouw	0.35	1.46	1.7	10.0	81,221	10,443
17	Sumajouw	0.35	2.10	1.7	9.9	80,786	11,023
18	Yost	0.00	0.93	0.0	5.0	81,221*	7571
19	Yost	0.00	0.93	0.0	5.0	81,221*	7934
20	Yost	0.00	0.93	0.0	5.0	81,221*	7890
21	Yost	0.40	3.00	1.0	5.0	81,221*	7600
22	Yost	0.40	3.00	1.0	5.0	81,221*	8195
23	Yost	0.40	3.00	1.0	5.0	81,221*	8253

Sources: Data from Sumajouw and Rangan (2006); Yost, Radlińska, Ernst, Salera, and Martignetti (2013).
Note: A_s = area of reinforcing steel in the tension zone; A_s' = area of reinforcing steel in the compression zone; d = distance from the extreme compression fiber to the centroid of the compression reinforcing steel group; d' = distance from the extreme compressive fiber to the centroid of the tension reinforcing group; f_c' = compressive strength of concrete; f_y = yield stress of steel reinforcing. 1 in. = 25.4 mm; 1 in.^{2} = 645 mm^2; 1 psi = 6.89 kPa.
* Values estimated using experimental data presented in Yost, Radlińska, Ernst, Salera, and Martignetti (2013).

dashed line in Fig. 7 represents ACI 318-14 specifications. Based on the results of these tests, the relationship shown in Eq. (17) is proposed to relate β_1 to f_c'.

$$\beta_1 = -(7 \times 10^{-5}) f_c' + 1.0783 \quad (17)$$

The values for α_1 and β_1 indicate that an equivalent rectangular stress block for geopolymer cement concrete materials is significantly smaller than similar blocks representing portland cement concrete behavior. The factor k_1 describes the ratio of the area defined by the parabolic stress distribution in Fig. 3 to the area of a rectangle fitted around its border. For a triangular distribution, the geometric factor would be 0.5, meaning that the triangle occupies half the area of the rectangle. Similarly, for parabolic distributions the appropriate factor is 0.67. The k_1 value for the geopolymer cement concrete materials was 0.54, indicating that the distribution at failure was nearly triangular.

The factor k_2 describes the distance of the resultant compression force C (defined in Fig. 3) from the extreme compressive fiber. The average computed value for k_2 was 0.25,

which indicates a strongly linear portion to the lower-strain portions followed by a softening near the upper-strain regions of the stress-strain relationship. This is apparent from the plots in Fig. 4.

Beam performance

Five reinforced geopolymer cement concrete beams were prepared with a subset (GCC1, GCC2, and GCC7) of the concrete mixture designs in Table 1. The beams were reinforced with no. 4 (13M) longitudinal bars and no. 3 (10M) closed stirrups. Each beam had the same reinforcing pattern of two bars in the compression zone and three in the tension zone. The actual yield stress of steel used in the beams was measured by a tension test of the reinforcing steel (**Table 3**). During the test, equal loads were applied at the third points of the 12 ft (3.65 m) span using a steel beam spreader. **Figure 8** shows the results of the beam tests, and **Table 4** gives the ultimate capacities.

The ultimate moments observed in the beams were similar to the moment capacity computed using provisions given in ACI 318-14, as interpreted in Eq. (18). Calculations to determine the equivalent Whitney stress block were conducted using indexed factors typically associated with portland cement concrete, including α_1 of 0.85 and β_1 of 0.85 for 3200 psi (22 MPa), 0.75 for 6000 psi (41 MPa), and β_1 of 0.65 for 11,900 psi (82.0 MPa) concrete. The actual yield strengths of the reinforcing steel for the GCC1, GCC2, and GCC4 beams were determined to be 82,000 psi (565 MPa), 90,000 psi (621 MPa), and 80,000 psi (552 MPa), respectively. These measured yield strengths were used in the calculations to estimate the design capacity of the reinforced concrete beams. Table 4 lists the ultimate moments (Fig. 8) observed in each of the beams. The existing formulas were capable of predicting the beam strength within just a few percentage points of measured values. Only specimen GCC1-beam 1 reached an ultimate moment that was slightly lower than its estimated moment capacity of 41.6 kip-ft (56.4 kN-m). Table 4 lists the calculated and observed cracking and ultimate moments in each of the beams.

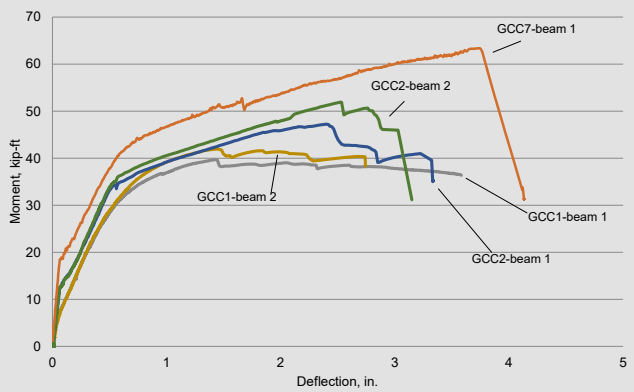

Figure 8. Moment-deflection responses for all beams. Note: 1 in. = 25.4 mm; 1 kip-ft = 1.356 kN-m.

The beam tests were also used to verify the applicability of the revised α_1 and β_1 parameters developed by testing the geopolymer cement concrete beam columns in flexure. The beam capacity calculated by Eq. (18) was estimated using Eq. (16) and (17) for α_1 and β_1.

$$M_n = {}_cC\left(d - \frac{a}{2}\right) + A_s^{'}E_s\varepsilon_s^{'}\left(d - d^{'}\right) \qquad (18)$$

M_n = nominal moment capacity of the beam

C_c = concrete compressive force

d = distance from the extreme compressive fiber to the centroid of the tension reinforcing group

a = depth of the equivalent rectangular stress block

$A_s^{'}$ = area of reinforcing steel in the compression zone

E_s = modulus of elasticity of reinforcing steel

$\varepsilon_s^{'}$ = strain at the centroid of the compression reinforcing steel group

$d^{'}$ = distance from the extreme compression fiber to the centroid of the compression reinforcing steel group

Table 4 shows the results. Because of the limited number of data points, as well as the fact that the beams have low reinforcement ratios, the improvement in capacity estimation accuracy is small compared with the α_1 and β_1 values provided by ACI 318-14. To test the revised parameters against a larger set of experimental results, Tables 3 and 4 present a meta-analysis of the beams reported by Yost et al.[9] and Sumajouw and Rangan.[8] The values in these tables were computed using specimen details for geometry, concrete compressive strength, and steel yield strength. The ultimate capacity of the beams was again estimated using α_1 and β_1 parameters defined in ACI 318-14. Two differences are notable between the estimated beam capacity presented in the original documents and the computed values in Table 3. First, Sumajouw and Rangan used provisions of AS 3600[11] to compute beam capacity,[8] while the work presented in this paper used ACI 318-14. Second, Yost et al. did not specifically measure the yield strength of the reinforcing steel used to construct the beams. Instead, capacity was computed using 60,000 psi (414 MPa) as the estimated yield strength of the reinforcing steel.[9]

As Sumajouw and Rangan and Yost et al. concluded, the existing equivalent stress-block parameters α_1 and β_1 yield satisfactory estimates of beam capacity. In research settings, where individual material characteristics and component geometries are known with good accuracy, the estimated capacity of the beam can usually be predicted

Table 4. Calculated and observed moments in flexural members

Beam	ρ	Measured ultimate capacity, lb-in.	Estimate using ACI 318-14, lb-in.	Difference from measured,* %	Capacity estimate using proposed k_1, k_2, k_3, lb-in.	Difference from measured,† %
1	0.0068	476,400	499,674	-4.9	497,801	-4.5
2	0.0068	502,800	499,674	0.6	497.801	1.0
3	0.0068	566,400	560,303	1.1	563,158	0.6
4	0.0068	559,200	560,303	-0.2	563,158	-0.7
5	0.0068	600,000	586,452	2.3	584,741	2.5
6	0.0065	498,297	401,352	19.5	403,284	19.1
7	0.0116	775,768	692,940	10.7	700,246	9.7
8	0.0183	1,034,210	1,026,386	0.8	1,042,946	-0.8
9	0.0266	1,420,545	1,338,066	5.8	1,362,995	4.1
10	0.0065	516,441	408,413	20.9	412,138	20.2
11	0.0116	801,435	705,517	12.0	712,241	11.1
12	0.0183	1,053,239	1,052,718	0.0	1,068,600	-1.5
13	0.0266	1,493,121	1,395,670	6.5	1,433,052	4.0
14	0.0065	574,413	427,203	25.6	427,768	25.5
15	0.0116	822,234	721,939	12.2	726,434	11.7
16	0.0183	1,122,275	1,081,472	3.6	1,093,527	2.6
17	0.0266	1,592,692	1,492,414	6.3	1,516,692	4.8
18	0.0154	288,001	257,660	10.5	260,652	9.5
19	0.0154	308,037	258,571	16.1	261,427	15.1
20	0.0154	313,271	258,466	17.5	261,337	16.6
21	0.0500	892,515	718,786	19.5	742,792	16.8
22	0.0500	859,242	729,813	15.1	752,504	12.4
23	0.0500	920,493	730,781	20.6	753,380	18.2

Note: k_1 = ratio of average compressive stress to maximum compressive stress; k_2 = ratio of distance from top of beam to the resultant compressive force C and the depth to the neutral axis c; k_3 = ratio of cylinder concrete strength to beam concrete strength; ρ = reinforcement ratio. 1 lb-in. = 0.113 N-m.

* Average error = 10.1%

† Average error = 9.3%

within 5% of the measured value. Sumajouw and Rangan attributed the great overestimate of strength for beams 6, 10, and 14 in Table 4 to the contribution of strain hardening, which is not accounted for in the model.[8,9]

The experimental results from the beam-column tests indicate that there are significant differences in the α_1 and β_1 parameters for geopolymer cement concrete and portland cement concrete. Using β_1 parameters devised for portland cement concrete could lead to an overestimate of geopolymer cement concrete beam strength. The underreinforced beams tested in this study do not exhibit this difference. At failure, the depth of the compression zone is small and the difference in different stress distributions is reduced.

Conclusion

Geopolymer cement concrete is a more sustainable building material that can be used as an alternative to portland

cement concrete. Fly-ash-based geopolymer cement concrete reduces carbon dioxide emissions and makes use of a waste byproduct from coal-burning power plants. Research on geopolymer cement concrete has shown that it can produce mixtures with similar mechanical properties to portland cement concrete, including compressive and flexural strengths, Poisson's ratio, and elastic modulus. Five flexural beam-column specimens were prepared and tested to evaluate the stress-strain relationship in the compression area of a flexural member. The beam-column specimens were subjected to axial and eccentric forces that simulate the compression stresses that occur in a beam in flexure.

Results from these tests indicate that the stress-strain response in geopolymer cement concrete behaves similarly to that of portland cement concrete. The stress-strain curve shows a positive linear slope in the elastic region. The slope decreases slightly as the ultimate strength is reached, and the stress reduces slightly before failure. Most of the tests in this research did not clearly show the post-peak response of the concrete, suggesting a rather brittle failure more typical of high-strength portland cement concrete. The results from these tests were used to evaluate the α_1 and β_1 parameters of the Whitney stress block, which were compared with the values provided in ACI 318-14. These were significantly different for geopolymer cement concrete, and their relationship has been expressed in terms of the compressive strength of concrete.

To verify the validity of these parameters, several flexural specimens were built and tested to failure. These beams were significantly underreinforced and had a relatively shallow compression block. Therefore, the improvement in estimating the ultimate flexural capacity is incremental. However, the ability to predict capacity would be improved for deeper or heavily reinforced members, as well as prestressed sections.

References

1. Hasanbeigi, A., L. Price, and E. Lin. 2012. "Emerging Energy-Efficiency and CO_2 Emission-Reduction Technologies for Cement and Concrete Production: A Technical Review." *Renewable and Sustainable Energy Reviews* 16 (8): 6220–6238.

2. Davidovits, J. 1991. "Geopolymers." *Journal of Thermal Analysis and Calorimetry* 37 (8): 1633–1656.

3. Duxson, P., J. L. Provis, G. C. Lukey, and J. S. J. van Deventer. 2007. "The Role of Inorganic Polymer Technology in the Development of 'Green Concrete.'" *Cement and Concrete Research* 37 (12): 1590–1597.

4. Turner, L. K., and F. G. Collins. 2013. "Carbon Dioxide Equivalent Emissions: A Comparison between Geopolymer and OPC Cement Concrete." *Construction and Building Materials* 43: 125–130.

5. McLellan, B. C., R. P. Williams, J. Lay, A. Van Riessen, and G. D. Corder. 2011. "Costs and Carbon Emissions for Geopolymer Pastes in Comparison to Ordinary Portland Cement." *Journal of Cleaner Production* 19 (9): 1080–1090.

6. Tempest, B., C. Snell, T. Gentry, M. Trejo, and K. Isherwood. 2015. "Manufacture of Full-Scale Precast Geopolymer Cement Concrete Components: A Case Study to Highlight Opportunities and Challenges." *PCI Journal* 60 (6): 39–50.

7. Van Deventer, J. S. J., J. L. Provis, and P. Duxson. 2012. "Technical and Commercial Progress in the Adoption of Geopolymer Cement." *Minerals Engineering* 29: 89–104.

8. Sumajouw, D., and B. Rangan. 2006. "Low-Calcium Fly Ash-Based Geopolymer Concrete: Reinforced Beams and Columns." Research report GC3, Curtin University of Technology, Perth, Australia.

9. Yost, J. R., A. Radlińska, S. Ernst, M. Salera, and N. J. Martignetti. 2013. "Structural Behavior of Alkali Activated Fly Ash Concrete. Part 2: Structural Testing and Experimental Findings." *Materials and Structures* 46 (3): 449–462.

10. ACI (American Concrete Institute) Committee 318. 2014. *Building Code Requirements for Structural Concrete (ACI 318-14)* and Commentary (ACI 318R-14). Farmington Hills, MI: ACI.

11. Standards Australia Committee BD-002. 2009. *Concrete Structures*. AS 3600-2009. Sydney, Australia: Standards Australia.

12. Prachasaree, W., S. Limkatanyu, A. Hawa, and A. Samakrattakit. 2014. "Development of Equivalent Stress Block Parameters for Fly-Ash-Based Geopolymer Concrete." *Arabian Journal for Science and Engineering* 39 (12): 8549–8558.

13. Hognestad, E., N. W. Hanson, and D. McHenry. 1955. "Concrete Stress Distribution in Ultimate Strength Design." *Journal of the American Concrete Institute* 52 (12): 455–480.

14. Davidovits, J. 2013. *Geopolymer Cement: A Review*. Saint-Quentin, France: Geopolymer Institute.

15. Sindhunata, J. S. J. van Deventer, G. C. Lukey, and H. Xu. 2006. "Effect of Curing Temperature and Silicate Concentration on Fly-Ash-Based Geopolymerization." *Industrial & Engineering Chemistry Research* 45 (10): 3559–3568.

16. Van Jaarsveld, J. G. S., J. S. J. van Deventer, and G. C. Lukey. 2002. "The Effect of Composition and Temperature on the Properties of Fly Ash- and Kaolinite-Based Geopolymers." *Chemical Engineering Journal* 89 (1–3): 63–73.

17. Diaz-Loya, E. I., E. N. Allouche, and S. Vaidya. 2011. "Mechanical Properties of Fly-Ash-Based Geopolymer Concrete." *ACI Materials Journal* 108 (3): 300–306.

18. Tempest, B. 2010. "Engineering Characterization of Waste Derived Geopolymer Cement Concrete for Structural Applications." PhD dissertation, University of North Carolina at Charlotte.

19. Thomas, R. J., and S. Peethamparan. 2015. "Alkali-Activated Concrete: Engineering Properties and Stress-Strain Behavior." *Construction and Building Materials* 93: 49–56.

20. Cross, D., J. Stephens, and J. Vollmer. 2005. "Structural Applications of 100 Percent Fly Ash Concrete." Paper presented at World of Coal Ash, Lexington, Ky.

21. Skipper, Ashley. 2014. "Performance of Geopolymer Cement Concrete in Flexural Members." Master's thesis, University of North Carolina at Charlotte.

22. Whitney, C. S. 1937. "Design of Reinforced Concrete Members under Flexure or Combined Flexure and Direct Compression." *Journal of the American Concrete Institute* 33 (3): 483–498.

Notation

a = depth of the equivalent rectangular stress block

a_1 = distance from the neutral face to P_1

a_2 = distance from the neutral face to P_2

A_s = area of reinforcing steel in the tension zone

A_s' = area of reinforcing steel in the compression zone

b = width of a rectangular concrete section

c = distance from the compressive face to the neutral axis in a concrete beam

C = resultant compressive force

C_c = concrete compressive force

d = distance from the extreme compression fiber to the centroid of the compression reinforcing steel group

d' = distance from the extreme compressive fiber to the centroid of the tension reinforcing group

e = eccentricity

E_c = elastic modulus of the concrete

E_s = modulus of elasticity of reinforcing steel

f = stress

f_0 = average stress on a cross section of the beam column

f_c = stress in the concrete

f_c' = compressive strength of concrete

f_y = yield stress of steel reinforcement

F = forces acting on the section of the beam column

h = depth of beam

k_1 = ratio of average compressive stress to maximum compressive stress

k_2 = ratio of distance from top of beam to the resultant compressive force C and the depth to the neutral axis c

k_3 = ratio of cylinder concrete strength to beam concrete strength

L = length of beams used in the experiments

m_0 = average moment acting on a section of the beam column

M = moment

M_n = nominal moment capacity of the beam

P_1 = primary axial load acting on the beam column

P_2 = eccentric load acting on the beam column

R^2 = coefficient of determination

w/cm = water–cementitious materials ratio

x = distance from neutral axis to the resultant compressive force line of action

α_1 = stress-block parameter = $\frac{k_1 k_3}{2k_2}$

β_1 = stress-block parameter = $2k_2$

ε = strain

ε_c = concrete strain

ε_s' = strain at the centroid of the compression reinforcing steel group

ε_x = linear distribution across c

ρ = reinforcement ratio

ρ_{bal} = reinforcement ratio at balanced failure conditions

ψ = factor fit to the data

About the authors

Brett Tempest, PhD, is an associate professor in the Department of Civil and Environmental Engineering at the University of North Carolina at Charlotte.

Janos Gergely, PhD, SE, PE, is an associate professor in the Department of Civil and Environmental Engineering at the University of North Carolina at Charlotte.

Ashley Skipper, MS, earned her master's degree from the Department of Civil and Environmental Engineering at the University of North Carolina at Charlotte.

Abstract

Geopolymer cement concrete could revolutionize the concrete industry by merging the benefits of concrete with significantly reduced greenhouse gas emissions compared with portland cement concrete. Several authors have verified the applicability of equivalent stress-block design parameters to estimating the capacity of reinforced geopolymer cement concrete beams. These verifications have been made primarily by testing small-dimension, underreinforced beams with fairly shallow compression zones. The research presented in this paper used a combined axial stress and flexure test developed by Hognestad et al. as a primary means of determining the distribution of stresses in the compression zone of geopolymer cement concrete in flexure. The results indicated that slightly modified stress block parameters α_1 and β_1 should be applied to geopolymer cement concrete due to differences in the stress-strain relationship of geopolymer cement concrete in compression compared with portland cement concrete. Although these parameters do not significantly improve the accuracy of calculations for small-dimension beams, they are more appropriate for general design conditions, which might include deeper beams, heavily reinforced sections, and prestressed sections.

Keywords

Beams, flexural design parameters, geopolymer cement concrete, greenhouse gas, sustainability, stress-strain curve.

Review policy

This paper was reviewed in accordance with the Precast/Prestressed Concrete Institute's peer-review process.

Reader comments

Please address reader comments to journal@pci.org or Precast/Prestressed Concrete Institute, c/o *PCI Journal*, 200 W. Adams St., Suite 2100, Chicago, IL 60606.